AN X-RAY PINHOLE CAMERA WITH A RANGE OF DEFINED APERTURES

Cyrille Thomas*, Guenther Rehm, Diamond, Oxfordshire, UK
Riccardo Bartolini, Diamond, Oxford University, Oxfordshire, UK

Abstract

Operation of 3^{rd} generation synchrotron light sources is heading towards low emittance coupling offering small vertical beam size and extending the transverse coherence of the X-ray photon beam. In the case of Diamond, exploring operation at 0.1% coupling will imply measuring vertical beam sizes of the order of 7μm (in bending magnets). Measurement of the vertical beam size and coupling with the best accuracy requires a precise knowledge of the Point Spread Function (PSF) of the electron beam imaging system. At Diamond two X-ray pinhole cameras are used for this measurement. In this paper we present our first results of beam size measurement using a deconvolution technique, based on the Lucy-Richardson iterative algorithm which uses the PSF of the imaging system. We verify the validity of the method with measurements of the electron beam size with a series of pinholes of well defined apertures varying from 12 to 100μm laser machined into a 200μm Tungsten plate. In this paper we discuss the experimental results and the accuracy of the method.

INTRODUCTION

Modern synchrotron radiation facilities are now heading towards operation with very small vertical coupling, typically several pm.rad. This implies that the vertical beam size is becoming smaller, and for the case of Diamond 0.1% coupling means a vertical beam size of 7.5 μm in the bending magnet and 3.3 μm at the center of the straight sections. Measuring such a small vertical beam size with minimal error is not trivial and requires a good knowledge of the measurement system. At Diamond we have two X-ray pinhole cameras located in bending magnets so that emittance, energy spread and vertical coupling can be measured at the same time. Besides, the sensitivity of the cameras allows to acquire images in typically 1 ms which shows some dynamical aspect of the transverse motion of the beam. The resolution of the X-ray pinhole camera has been shown [1] to be good enough to allow beam size measurement down to 6 μm. However, it has been shown that the quadratic subtraction could over evaluate the beam size by up to 40% [1]. To compensate for this potential error we have been applying a full image deconvolution technique. In order to investigate this, we have installed a series of pinholes of circular apertures from 5 μm to 100 μm diameters. Using theses pinholes, we have been measuring the beam size in both axes with all the pinholes, and varied the vertical coupling between 0.1% and 0.3%. In the following, we present the experimental results and the analysis of the images using the Lucy-Richardson deconvolution algorithm. For the technique to be validated, the results should be consistent showing a unique converging beam size for the same lattice parameters and also should verify physics law as for example shown here the proportionality between the vertical beam size and the touschek lifetime.

BEAM SIZE MEASUREMENT

The two X-ray pinhole cameras at Diamond image the electron beam from two bending magnets. The X-ray beam has a spectrum from 15 keV to over 60 keV peaking around 26 keV. The position of the pinholes is such that the magnification (geometrical) is 2.4 and 2.7 for pinhole 1 and 2 respectively. More details about the pinholes can found in [1]. In the main configuration, the pinholes are square of nominal apertures of 25 μm. We add to this configuration a 200 μm thick Tungsten plate in which laser ablated pinholes are positioned in line all separated by 1 mm. The optically measured diameter of each pinhole are 5, 12, 12, 20, 25, 30, 50, and 100 μm [1]. It is possible to insert either the square or circular pinholes with a horizontal linear translation stage. For the measurement to be done, we have injected 100 mA in the storage ring with the nominal lattice. LOCO measurement [2] has been performed and applied to set a very small coupling, K = 0.12%, as part of a regular and well controlled operation routine. Images of the beam at the same coupling and the same current have then been acquired for all pinholes. Each image is first fit with a 2-D Gaussian distribution retrieving the raw image beam size, and then deconvolved using the Lucy-Richardson deconvolution algorithm [3, 4], which gives the most-likelihood image deconvolved by the given PSF. The beam size of the deconvolved image has also been retrieved by a fit with a 2-D Gaussian distribution.

For each pinhole the PSF has been generated using the Fresnel diffraction integral, taking into account the intensity spectrum at the scintillator LuAG screen of the X-ray camera, the spectral intensity yield of the LuAG screen and finally the camera resolution. The synchrotron radiation in the LuAG screen is filtered by 8 mm of Al and air across the distance pinhole-screen. The LuAG spectral intensity yield is $20 \cdot 10^3$ph / MeV [2]. The Fresnel diffraction integral for the pinhole parameters is calculated for each photon wavelength of the power spectrum and summed up with its normalised intensity [1]. Then the image obtained is

* cyrille.thomas@diamond.ac.uk

[1] the targeted circular apertures were 5, 10, 15, 20, 25, 30, 50 100 μm
[2] http://www.crytur.cz/files/editor/file/import/LuAG_Ce.pdf

ISBN 978-3-95450-121-2

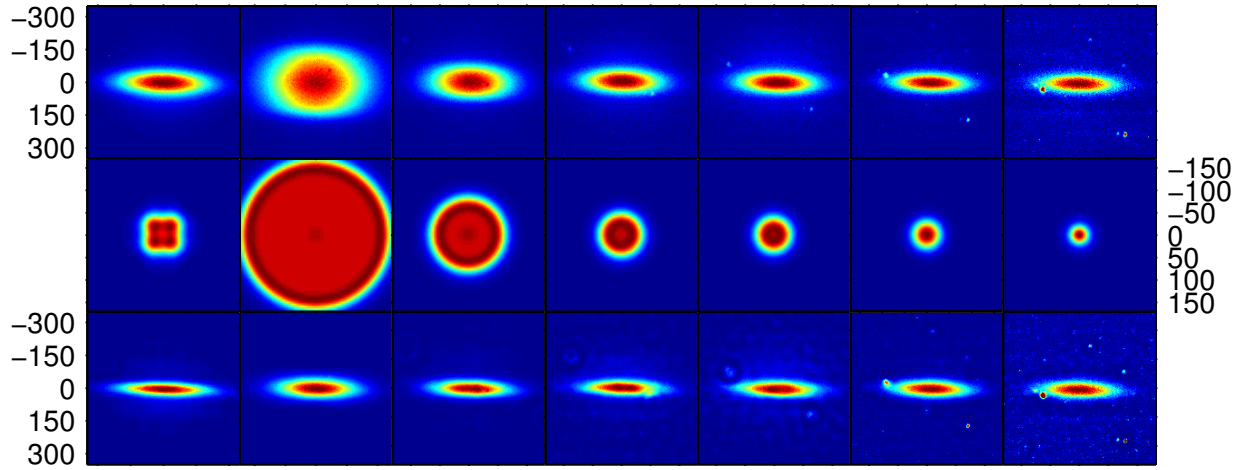

Figure 1: Top: Images of the beam at pinhole 1 with the nominal 25 μm aperture first from the left and 100, 50, 30, 25, 20, 12 μm circular pinholes. The background from the transmitted X-rays through the 0.2 mm thick tungsten plate has been subtracted. Middle: The PSF of the X-ray pinhole. Bottom: same images as above but after deconvolution. The axis are equal and in micrometers but the scale for the PSFs is two times larger than for the beam images.

convolved with a 2D-Gaussian distribution that takes into account the X-ray camera PSF. It is assumed that the image of the source formed by the pinhole on the screen is incoherent.

We repeated the operation with increased coupling 0.2% and 0.3%, measured with our standard routine calculation.

Deconvolution

The deconvolution we apply to the image is performed in Matlab, and is based on the Lucy-Richardson algorithm [3,4], which is an iterative procedure for recovering a latent image that has been blurred by a known point spread function. When the iteration converges, it converges to the maximum likelihood solution [5]. The deconvolved image is then the most probable image representing the object. Figure 1 presents images of the beam at pinhole 1 and for our square pinhole and 6 of the circular pinholes together with the deconvolved images. In the middle we have shown the image of the calculated PSF in each case in a larger scale so that all the PSF can be appreciated. The raw images taken with the circular pinholes have had the background due to transmission through the 200 μm Tungsten removed. As a results the dynamic range of the images is limited, in particular for the smallest aperture where the signal is hardly above the background and is comparable to the noise.

The PSF is dependant on the aperture of the pinhole, but also on the distances source-pinhole and pinhole-X-ray camera. The distances have been measured with a good accuracy, and although the apertures have been measured optically by the company making the circular apertures, we have investigated the sensitivity to a small variation of the aperture diameter. To this end, we have deconvolved the images with varying the aperture sizes ± 2 μm around their measured size. For the square pinhole sizes, they are made with shims but still carry an uncertainty due to the compression of the assembly and their position and orientation in the beam as they are more than 10 mm long and thus any tilt will close the aperture.

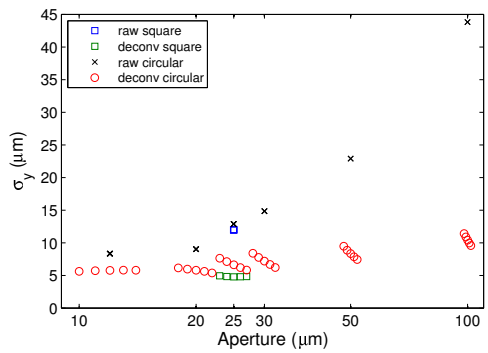

Figure 2: Vertical beam sizes (at Pinhole 1) measured by 2-D Gaussian fit of the raw and deconvolved images, K=0.12, as function of the pinholes aperture. For each pinhole the PSF has been calculate using an aperture varying ± 2 μm in steps of 1 μm from the optically measured one.

Experimental Results

For the 3 coupling set values, beam sizes have been measured on raw images and on deconvolved images by a 2-D Gaussian fit. Figure 2 presents the results comparing the vertical beam sizes from raw and deconvolved images and for K = 0.12. The deconvolved beam sizes for all apertures tend to converge towards the same value. Here, although the unique beam size is not absolutely known, it appears after deconvolution to be of the order of 5 to 7 μm. Depending on the pinhole aperture, the deconvolved vertical beam size is smaller than the beam size measured on the raw images by a factor 1.6 to 4.5. Conversely, the horizon-

ISBN 978-3-95450-121-2

Table 1: Beam horizontal and vertical sizes measured after deconvolution for both pinholes at the coupling emittance K = 0.12% and for all apertures (A)- square (s) and circular (c). The variation $\Delta\sigma_{i,j}$ indicates the half-difference between the extremum values for the aperture varying ± 2 μm around the optically measured one.

A (μm)	$\sigma_{x,1} \pm \Delta\sigma_{x,1}$	$\sigma_{x,2} \pm \Delta\sigma_{x,2}$	$\sigma_{y,1} \pm \Delta\sigma_{y,1}$	$\sigma_{y,2} \pm \Delta\sigma_{y,2}$
25 (s)	55.9 ± 0.15	48.1 ± 0.1	4.8 ± 0.08	6.2 ± 0.6
100 (c)	55.3 ± 0.7	45.8 ± 0.35	10.4 ± 0.9	12.3 ± 1.2
50 (c)	54.6 ± 0.4	48.0 ± 0.2	8.4 ± 1.0	8.3 ± 0.8
30 (c)	55.2 ± 0.2	46.9 ± 0.2	7.2 ± 1.0	7.4 ± 1.0
25 (c)	55.8 ± 0.16	44.6 ± 0.25	6.7 ± 0.9	7.8 ± 0.4
20 (c)	52.4 ± 0.3	44.3 ± 0.2	5.8 ± 0.4	6.1 ± 0.2
12 (c)	52.7 ± 0.1	44.1 ± 0.1	5.7 ± 0.1	7.1 ± 0.1

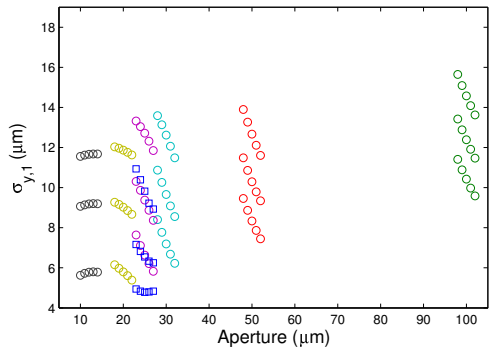

Figure 3: Vertical beam sizes (at Pinhole 1) measured by 2-D Gaussian fit of the deconvolved images, and for 3 coupling values (K=0.12, 0.20, 0.32), as function of the pinholes aperture varied by ± 2 μm in steps of 1 μm. For each pinhole the beam size increases with increasing coupling.

tal sizes should all be the same. However, as summarised in the table 1 the differences found in both planes show a standard deviation of the order of 2% and 15% in the horizontal and vertical planes respectively. Looking closer at the deconvolved vertical beam sizes for the three coupling values, Fig. 3, the variation of the aperture size seems to indicate some of the apertures are likely to be smaller or larger than indicated. For instance, the square nominal 25 μm pinhole is likely to be 20 μm, whereas the 30 μm would likely be 35 μm. This shows the importance in the knowledge of the PSF.

Vertical Beam Size and Touschek Lifetime

The beam size retrieved by deconvolution has to be proportional to the Touschek lifetime. Figure 4 shows all the vertical beam sizes after deconvolution on both pinholes against the measured lifetime corrected using 55h gas lifetime [6], which should correspond to the Touschek lifetime. Data from all seven apertures can be fit with a 1st order polynomial, from which a 50% interval confidence is found to be 10% on average of the measured values.

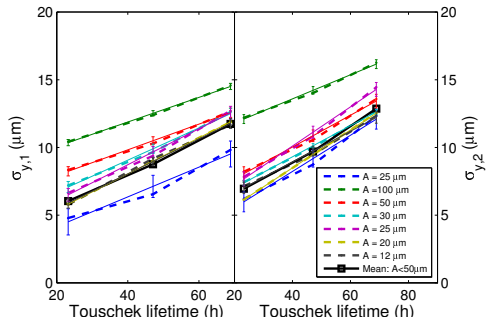

Figure 4: Vertical beam sizes on both pinholes as function of the Touschek lifetime. The line and error-bars are generated by a linear fit.

CONCLUDING REMARKS

The image deconvolution technique applied for the measurement of the beam size with X-ray pinhole camera can extend the capability of measuring very small beam sizes several times smaller than the raw resolution of the imaging system. For the case of Diamond, this technique should allow measurement of vertical beam size at the smallest possible vertical emittance coupling. However, further investigation of the method is required for it to be fully validated. The variability of the deconvolved vertical beam sizes illustrates the essential need of a precise knowledge of the transmission profile of the aperture as seen by the X-rays.

REFERENCES

[1] Cyrille Thomas, Guenther Rehm, and Ian Martin. X-ray pinhole camera resolution and emittance measurement. *Physical Review Special Topics - Accelerators and Beams*, 13(2):1–11, February 2010.

[2] J. Safranek, G. Portmann, A. Terebilo, and C. Steier. MATLAB-BASED LOCO. In *Proceedings of EPAC*, pages 404–406, 2002.

[3] W. H. Richardson. Bayesian-based iterative method of image restoration. *J. Opt. Soc. Am.*, 62(1):55–59, Jan 1972.

[4] L. B. Lucy. An iterative technique for the rectification of observed distributions. *Astronomical Journal*, 79:745, June 1974.

[5] L. A. Shepp and Y. Vardi. Maximum likelihood reconstruction for emission tomography. *Medical Imaging, IEEE Transactions on*, 1(2):113 –122, oct. 1982.

[6] I. Martin. Lifetime measurements for the diamond storage ring. Technical Report AP-SR-REP-0150, DLS, Feb 2007.

ISBN 978-3-95450-121-2